Using Unfolding Techniques to Separate Charm and Bottom Contributions to Single Electron Yields from Semi-leptonic Decays of Heavy Flavor Hadrons Measured by PHENIX

D. McGlinchey (for the PHENIX Collaboration)
University of Colorado Boulder

Unfolding method

In [1], we apply Bayesian inference techniques to the problem of separating electrons from charm and bottom hadron decays using measured distributions of electron DCA_T and p_T.

Given a vector of measured data, $\mathbf{x}$, and a vector of model parameters, $\boldsymbol{\theta}$, we use Bayes' theorem

$$p(\boldsymbol{\theta}|\mathbf{x}) = \frac{P(\mathbf{x}|\boldsymbol{\theta})\pi(\boldsymbol{\theta})}{P(\mathbf{x})}, \tag{1}$$

to compute the posterior probability density $p(\boldsymbol{\theta}|\mathbf{x})$ from the likelihood $P(\mathbf{x}|\boldsymbol{\theta})$ and prior information $\pi(\boldsymbol{\theta})$. The denominator $P(\mathbf{x})$ serves as an overall normalization of the combined likelihood $P(\mathbf{x}|\boldsymbol{\theta})\pi(\boldsymbol{\theta})$ such that $p(\boldsymbol{\theta}|\mathbf{x})$ can be interpreted as a probability density.

Here $\boldsymbol{\theta}$ consists of 17 bins in p_T of both charm and bottom hadron yields. We employ an affine-invariant ensemble sampler described in Ref. [2] to draw samples of $\boldsymbol{\theta}$ in proportion to $p(\boldsymbol{\theta}|\mathbf{x})$.

Modeling the likelihood function

This analysis is based on 21 data points of total heavy flavor electron invariant yield, $\mathbf{Y}^{\text{data}}$, in the range 1.0-9.0 GeV/c from the 2004 data set [3], and five electron DCA_T distributions $\mathbf{D}_j^{\text{data}}$, where j indexes each electron p_T (p_T^e) interval within the range 1.5-5.0 GeV/c from the 2011 data set. Therefore,

$$\mathbf{x} = (\mathbf{Y}^{\text{data}}, \mathbf{D}_0^{\text{data}}, \mathbf{D}_1^{\text{data}}, \mathbf{D}_2^{\text{data}}, \mathbf{D}_3^{\text{data}}, \mathbf{D}_4^{\text{data}}). \tag{2}$$

For each trial set of hadron yields, the prediction in electron p_T, $\mathbf{Y}(\boldsymbol{\theta})$, and DCA_T, $\mathbf{D}_j(\boldsymbol{\theta})$, is calculated by

$$\mathbf{Y}(\boldsymbol{\theta}) = \mathbf{M}^{(\mathbf{Y})}\boldsymbol{\theta}_c + \mathbf{M}^{(\mathbf{Y})}\boldsymbol{\theta}_b \tag{3}$$

$$\mathbf{D}_j(\boldsymbol{\theta}) = \mathbf{M}_j^{(\mathbf{D})}\boldsymbol{\theta}_c + \mathbf{M}_j^{(\mathbf{D})}\boldsymbol{\theta}_b, \tag{4}$$

where $\mathbf{M}^{(\mathbf{Y})}$ and $\mathbf{M}_j^{(\mathbf{D})}$ are decay matrices (discussed later). The (log) likelihood between the prediction and each measurement in the datasets $\mathbf{Y}^{\text{data}}$ and $\{\mathbf{D}_j^{\text{data}}\}_{j=0}^{4}$ is then evaluated using

$$\ln P(\mathbf{x}|\boldsymbol{\theta}) = \ln P(\mathbf{Y}^{\text{data}}|\mathbf{Y}(\boldsymbol{\theta})) + \sum_{j=1}^{5} \ln P(\mathbf{D}_j^{\text{data}}|\mathbf{D}_j(\boldsymbol{\theta})). \tag{5}$$

The likelihood $\ln P(\mathbf{Y}^{\text{data}}|\mathbf{Y}(\boldsymbol{\theta}))$ is modeled as a multivariate Gaussian with diagonal covariance. The likelihood $\ln P(\mathbf{D}_j^{\text{data}}|\mathbf{D}_j(\boldsymbol{\theta}))$ is described by a multivariate Poisson distribution, as the DCA_T data is in counts.

Decay model and matrix normalization

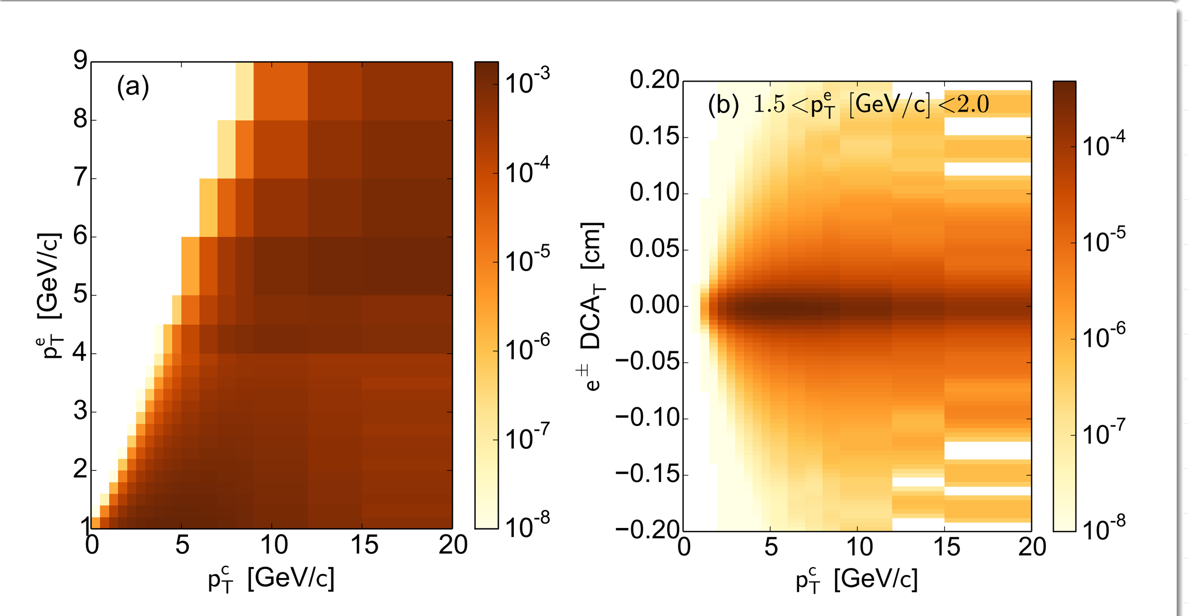

Figure 1: (a) The decay matrix, $\mathbf{M}^{(\mathbf{Y})}$, encoding the probability for charmed hadrons decaying to electrons within $|\eta| < 0.35$ as a function of both p_T^e and charm hadron p_T (p_T^c). (b) An example decay matrix, $\mathbf{M}_j^{(\mathbf{D})}$, encoding the probability for charmed hadrons decaying to electrons within $|\eta| < 0.35$ and $1.5 < p_T^e$ [GeV/c] < 2.0 as a function of both electron DCA_T and p_T^c.

They PYTHIA-6 generator with forced heavy flavor production (MSEL=4,5) is used to generate parent charm (bottom) hadrons and their decays to electrons. Electrons within $|\eta| < 0.35$ decayed from the ground state charm hadrons ($D^{\pm}$, D^0, D_s, and Λ_c) or bottom hadrons ($B^{\pm}$, B^0, B_s, and Λ_b) are used to create a decay matrix between hadron p_T and electron p_T and DCA_T. Here we treat the feed down decay $B \to D \to e$ as a bottom hadron decay and exclude it from charm hadron decays.

Regularization/prior

Discontinuities in the unfolded distributions of charm and bottom hadron yields are penalized by including the regularization term

$$\ln \pi(\boldsymbol{\theta}) = -\alpha^2 \left(|\mathbf{L}\mathbf{R}_c|^2 + |\mathbf{L}\mathbf{R}_b|^2\right) \tag{6}$$

where $\mathbf{R}_c$ and $\mathbf{R}_b$ are ratios of the charm and bottom components of the parent hadron p_T vector to the corresponding 17 components of the prior, $\boldsymbol{\theta}_{\text{prior}}$, and $\mathbf{L}$ is a 17-by-17 second-order finite-difference matrix. Thus the addition of this term encodes the assumption that departures from $\boldsymbol{\theta}_{\text{prior}}$ should be smooth by penalizing total curvature as measured by the second derivative. Here, $\alpha = 1.0$ and $\boldsymbol{\theta}_{\text{prior}}$ is set to PYTHIA charm and bottom hadron p_T distributions scaled by a modified blast wave calculation [4].

Correlations between parent charm and bottom hadron yields

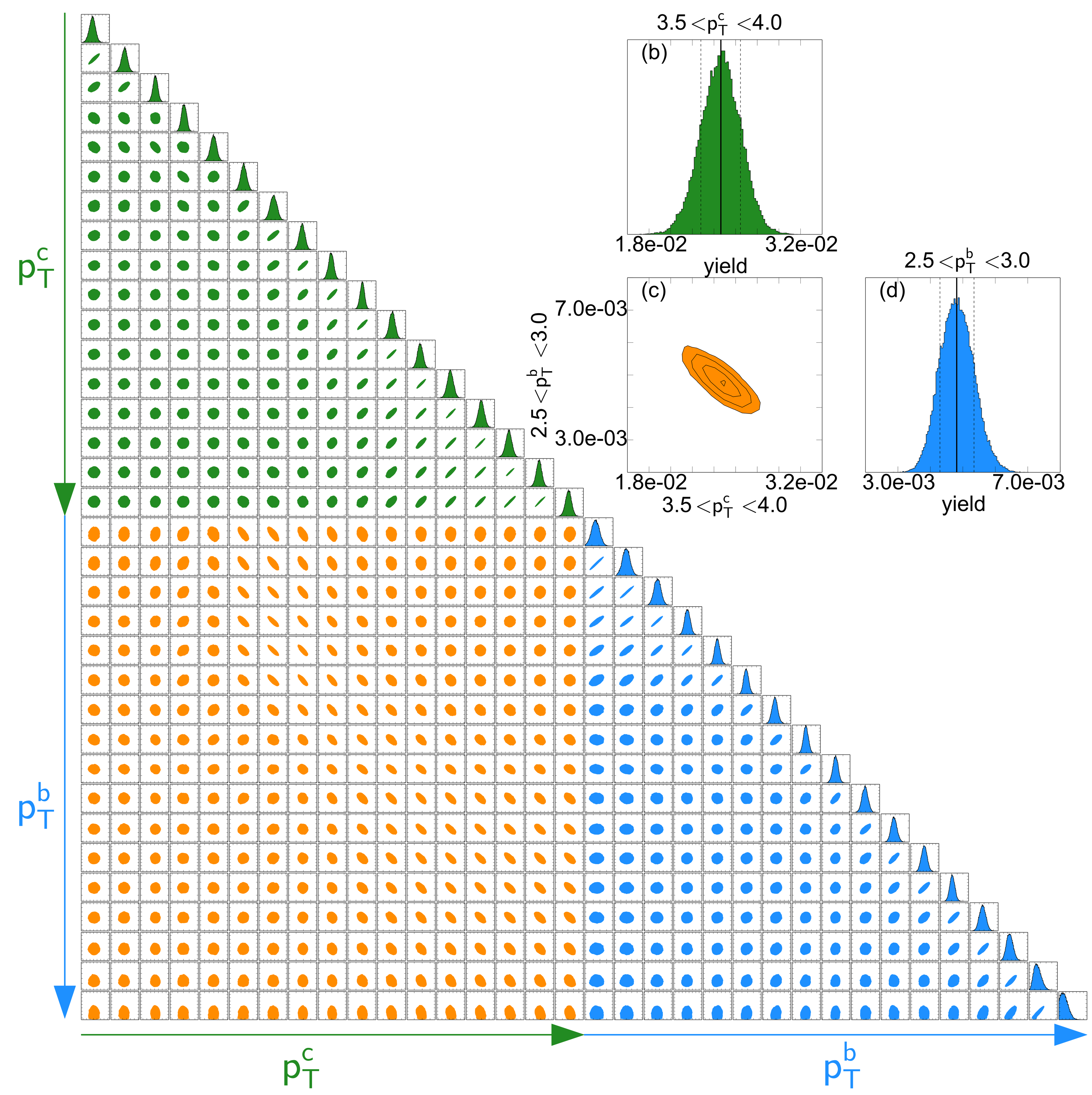

Figure 2: The joint probability distributions for the vector of hadron yields, $\boldsymbol{\theta}$, showing the 2-dimensional correlations between parameters. The diagonal plots show the marginalized probability distributions for each hadron p_T bin (i.e. the 1 dimensional projection over all other parameters). Along the Y-axis the plots are organized from top to bottom as the 17 charm hadron p_T (p_T^c) bins from low to high p_T^c followed by the 17 bottom hadron p_T (p_T^b) bins from low to high p_T^b. The X-axis is organized similarly from left to right. The p_T^c and p_T^b binning follows that shown in Fig. 5. The region of green (blue) plots shows the correlations between charm (bottom) hadron yields. The region of orange plots shows the correlations between charm and bottom hadron yields. A circular contour in the 2-dimensional panels represents no correlation between the corresponding hadron p_T bins. An oval shape with a positive slope indicates a positive correlation between corresponding bins, and an oval shape with a negative slope represents an anti-correlation between corresponding bins. Sub-panels (b)-(d) show a set of example distributions.

A large positive correlation is seen for adjacent bins in Fig. 2 for high-p_T charm hadrons and low-p_T bottom hadrons. This is a consequence of the regularization, which requires a smooth p_T distribution, and is stronger where there is less constraint from the data. There is also a region of anti-correlation between the mid to high p_T charm hadrons and the low to mid p_T bottom hadrons. Charm and bottom hadrons in these regions contribute decay electrons in the same p_T region, and appear to compensate for each other to some extent.

Re-folded comparisons to data

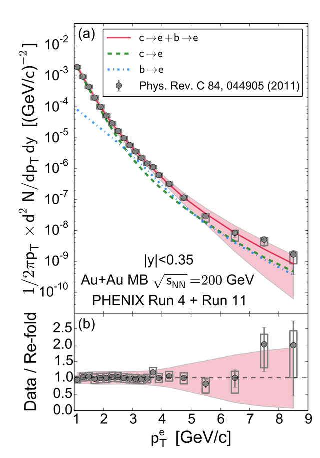

Figure 3: The heavy flavor electron invariant yield as a function of p_T [3] compared to electrons from the re-folded charm and bottom hadron yields.

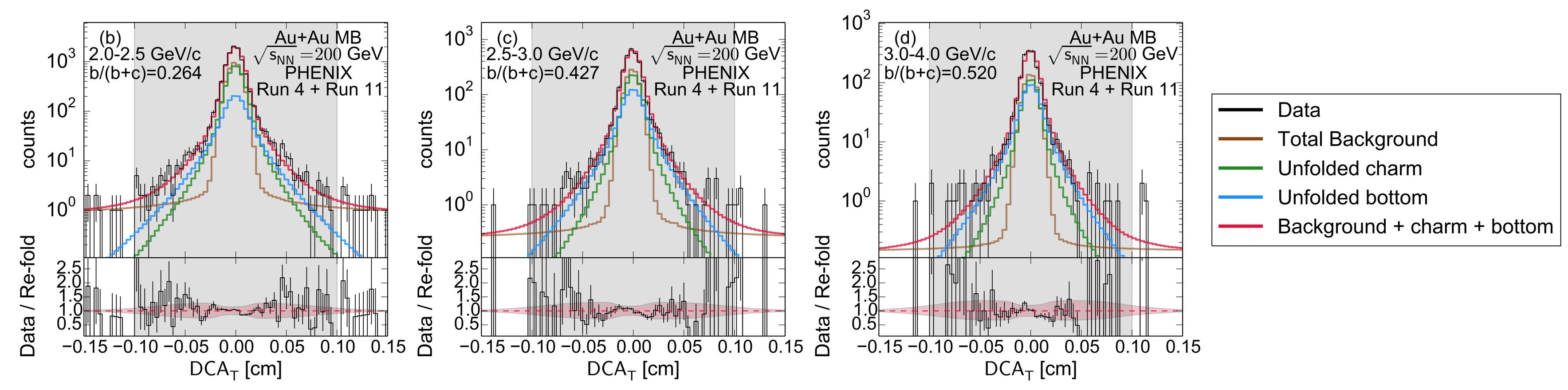

Figure 4: The DCA_T distribution for measured electrons compared to the decomposed DCA_T distributions for background components, electrons from charm decays, and electrons from bottom decays. The gray band indicates the region in DCA_T considered in the unfolding procedure. See Ref. [1] for all DCA_T comparisons.

Results

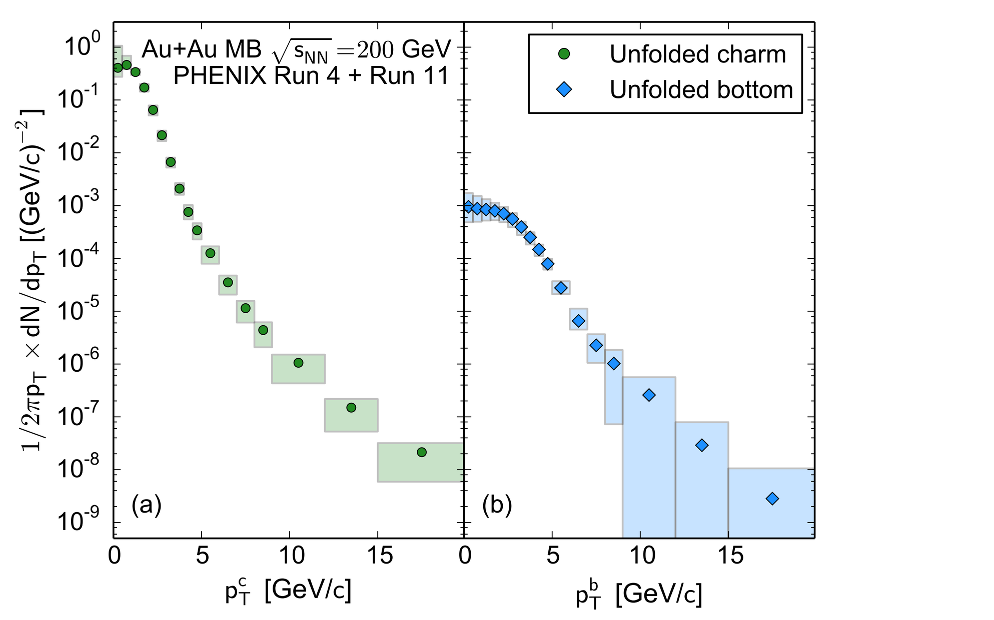

Figure 5: Unfolded charm and bottom hadron invariant yield as a function of p_T, integrated over all rapidities, as constrained by electron yield vs DCA_T in 5 p_T bins and previously published heavy flavor electron invariant yield vs p_T [3].

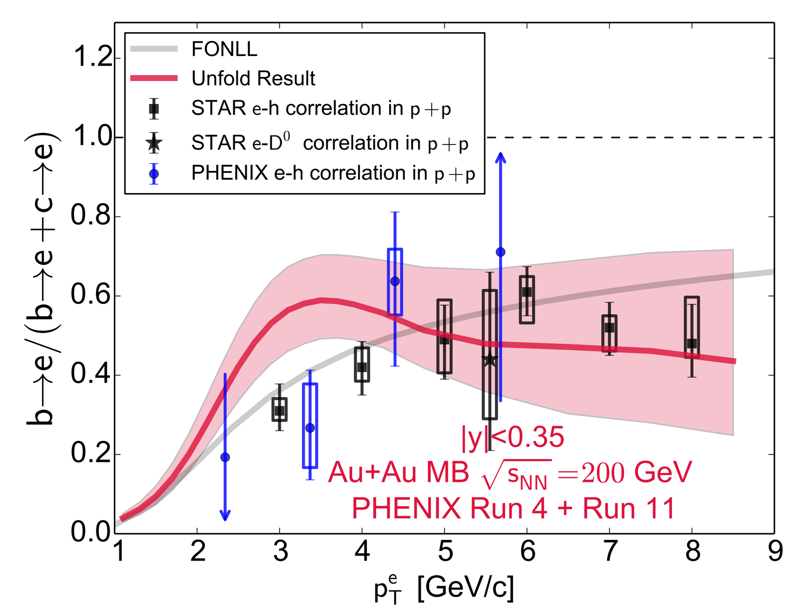

Figure 6: The Bottom electron fraction as a function of p_T^e compared to measurements in p+p collisions at $\sqrt{s}$ =200 GeV from PHENIX [5] and STAR [6], as well as the central values for FONLL [7] for p+p collisions at $\sqrt{s_{NN}}$ =200 GeV.

Also see posters by **T. HACHIYA**, **H. ASANO**, and **K. NAGASHIMA**.

Acknowledgments

We acknowledge funding support from the United States Department of Energy Division of Nuclear Physics grant DE-FG02-00ER41152.

References

[1] A. Adare et al. 2015, arXiv:1509.04662.

[2] D. Foreman-Mackey, D. W. Hogg, D. Lang, and J. Goodman. *Publications of the Astronomical Society of the Pacific*, 125:306–312, March 2013.

[3] A. Adare et al. *Phys.Rev.*, C84:044905, 2011.

[4] Andrew M. Adare, Michael P. McCumber, James L. Nagle, and Paul Romatschke. *Phys.Rev.*, C90(2):024911, 2014.

[5] A. Adare et al. *Phys.Rev.Lett.*, 103:082002, 2009.

[6] M.M. Aggarwal et al. *Phys.Rev.Lett.*, 105:202301, 2010.

[7] Matteo Cacciari, Paolo Nason, and Ramona Vogt. *Phys.Rev.Lett.*, 95:122001, 2005.

darren.mcglinchey@colorado.edu

QUARK MATTER 2015
The XXVth International Conference on Ultrarelativistic Nucleus-Nucleus Collisions